

# Method to Measure Radial Thermal Conductivity for Cylindrical Samples

Jiahuan He,\* Long Wen, Xiao He, Tingting He, Tangyan Liu, Qiang Kang, Daocheng Wang, Xian Peng, Hongyu Yao, Yin Zhang, and Xiaohang Deng



Cite This: *ACS Omega* 2023, 8, 6530–6537



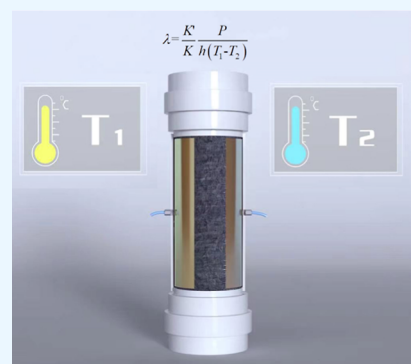
Read Online

ACCESS |

Metrics & More

Article Recommendations

**ABSTRACT:** Anisotropy is a prevailing property in most substances in the real world. The thermal conductivity characteristic of anisotropy must be determined for utilizing geothermal resources and assessing battery performances. Most core samples were primarily obtained by drilling and intended to be cylindrical in shape, with the cores resembling quantities of familiar batteries. Although Fourier's law could be used to measure the axial thermal conductivity of square or cylindrical samples, there is still a need to develop a new method to measure the radial thermal conductivity of cylindrical samples and evaluate their anisotropy. Thus, we established a testing method for cylindrical samples using the theory of complex variable functions following the heat conduction equation and implemented a numerical simulation to determine the difference between this method and typical ones via a finite element model for various samples. Results show that the method could perfectly gauge the radial thermal conductivity of cylindrical samples with more powerful availability.



## 1. INTRODUCTION

In 2021, the State Council of China unveiled the Action Plan for Carbon Peaking by 2030. Because the issue of climate change has become relevant to all humanity, traditional petroleum companies have been exploring the promotion and transition of their energy structure. Simultaneously, experimenting with new ideas has been prioritized, particularly exploiting recent technological advancements for low-carbon and green new energy resources except for oil and gas.<sup>1–3</sup> Oil giants have shifted their focus one after another owing to the transition wave, with Total replaced by TotalEnergies and BP by Beyond Petroleum. China National Petroleum Corporation has also set an exploitation goal focusing on oil, gas, geothermal energy, power, and hydrogen.<sup>4,5</sup>

All nations must achieve the carbon neutrality goal by 2065–2070 following the requirements of the Paris agreement. European and American countries place a premium on technological approaches toward low-carbon energy resources.<sup>6,7</sup> The cleanliness of geothermal attracts considerable attention, and its available exploitation tools, such as those for oil and gas, are crucial considerations for petroleum companies in the transition course.<sup>8–10</sup> As predicted by the International Energy Agency, the installed power-generating capacity of global geothermal resources will reach 150 GW in 2050 and exceed 250 GW in 2100, amounting to approximately 3.5% of the world's energy supply. Besides geothermal power generation, an enhanced geothermal system based on volume fracturing technology may be employed as another approach

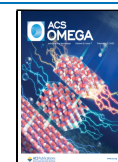
for exploiting geothermal resources.<sup>11–13</sup> Researchers have considered using the resources from abandoned oil and gas wells.<sup>14</sup>

Anisotropy is a universal physical property prevailing in common materials or media. Substantial anisotropic differences exist among crystals, various materials used in daily life, and earth media.<sup>15–17</sup> The industry is well aware of the importance of thermal conductivity anisotropy in geothermal exploitation. Geophysicists have focused their attention on this anisotropy in rocks. Safanda et al. used a numerical solution to express the effects of thermal conductivity anisotropy via building a two-dimensional (2D) anisotropy model of rocks in a geothermal field.<sup>18</sup> Both Deming et al. and Pribnow et al. developed experimental approaches for testing thermal conductivity in both cuttings and core samples at room temperature.<sup>19,20</sup> It is essential to clarify thermal conductivity during the exploitation of geothermal resources, especially for scheme design and numerical simulation. The battery will generate some heat during use, and the anisotropy of thermal conductivity may act on its properties. So, it is of great importance to explore this parameter for battery manufacturing

**Received:** October 26, 2022

**Accepted:** January 27, 2023

**Published:** February 10, 2023



fields. The issue of thermal conductivity anisotropy in porous media is not limited to one petrological domain.

## 2. PROBLEM STATEMENT

Testing approaches for assessing radial thermal conductivity in rocks are less suitable for assessing the performance of cylindrical batteries. Steady-state heat flow meter, guarded hot plate, circular tube, non-steady-state hot wire, and flash transient plane source are all commonly used methods designed for regular samples, particularly with planar surfaces, according to testing requirements.<sup>21,22</sup> The thermal conductivity of cylindrical samples is commonly measured by touching one of their flat sides to a heat source and calculating the amount of heat output from the opposite side. However, determining the thermal conductivity of cylindrical samples in other directions is difficult owing to their anisotropic nature. To measure this conductivity, Carmona et al. developed a technique of the heat source, namely, the center input and the radial output. This technique yielded vague conductivity values but could not reflect these values at different angles or in various directions.<sup>23</sup> Drake et al. and Muhammad et al. proposed another gauging method based on heat-insulating unsteady heating, which possessed an effective nondestructive merit in battery testing.<sup>24,25</sup> However, it only provided a broader perspective and failed to display the radial thermal conductivity at different angles; moreover, the representative anisotropy had both conventional axial and generalized radial orientations.

The vast majority of cores are cylindrical as they are sampled via drilling.<sup>26</sup> Different from rocks that can be cut into various shapes, the cylindrical batteries only as the whole may have their own functional characteristics. Furthermore, assessing the thermal conductivity anisotropy of cylindrical batteries via special preparation, such as wire cutting, is less likely. Nondestructive testing is surely for electronic goods that must retain their shape to be functional.<sup>14,21,27</sup> To summarize, a method must be developed to test the radial thermal conductivity for cylindrical samples, which can be used to evaluate geothermal resources as well as explore, develop, and use hot and dry rocks and assess the performance of cylindrical batteries.

## 3. THEORETICAL BASIS AND EXPERIMENTS

This method is similar to the radial measurement of core permeability and radial resistivity testing.<sup>26,28</sup> As shown in Figure 1, two curved metals with a specific arc-centering angle are placed on the arcuate surface of one cylindrical sample, with the left side serving as the heat source plate and the right side serving as the heat dissipation plate; moreover, another space beyond the metals is equipped with a thermal-insulating layer to prevent heat loss to the maximum extent.

Unlike calculation via direct application of a linear law, the heat conductivity test is difficult, as shown in Figure 1. Because the plane has become a curved surface, such a problem cannot be solved directly using a simple formula involving elementary calculations. Researchers have used conformal transformation in complex variable functions to solve the abovementioned issues and successfully applied seepage and electric conduction problems in the past.<sup>26,30</sup> Fortunately, the thermal conductivity also satisfies the partial differential equation  $\partial u/\partial t = k\nabla u$ . As long as the properties of the sample in a certain direction are the same and the Cauchy–Riemann condition is satisfied in

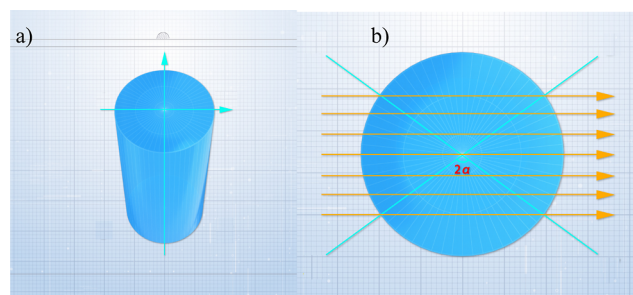


**Figure 1.** Heat flow along the diameter direction of the core. (a) Cylindrical sample with  $S$  as its cross-sectional area and  $L$  as the length, (b) heat passing the curved heat source and heat dissipation plates through the cross section of the sample; temperatures on the left and right sides being represented by  $T_1$  and  $T_2$ , respectively, and the centripetal angle of the two plates denoted as  $\beta$  equaling to  $(\pi - 2\alpha)$ .

the 2D plane, conformal transformation similar to that used in seepage and electricity conduction can be adopted. Muskat et al. and He et al. proposed the total 2D flux for the given geometry and boundary conditions.<sup>26,29,30</sup> The derivation content of this part is relatively complex, necessitating a lot of space, and similar issues have been discussed by Muskat et al. and He et al. Hence, each derivation process is not discussed in the current study. The derivation process can be performed by replacing the physical quantity used to express pressure or electric potential with temperature and similarly changing permeability or electrical conductivity into thermal conductivity. A similar conclusion can be drawn.

Figure 2 depicts the derivation process. Figure 2a refers to the one-fourth circle selected for consideration in Figure 1b. Clearly, other one-fourth circles have some degree of symmetry. Figure 2b shows the transformed domain obtained via conformal transformation. Figure 2c depicts the extension of the transformed domain by the Schwarz–Christoffel transformation.

Similar to seepage and resistivity issues, a formula for the radial thermal conductivity of cylindrical samples can be obtained as follows

$$\lambda = \frac{K'P}{Kh(T_1 - T_2)} \quad (1)$$

where  $K'$  and  $K$  refer to the complete elliptic integral of the first kind with modulus  $\sin\alpha$  and  $\cos\alpha$ , respectively. Figure 3 depicts the experimental procedures for this testing.

## 4. EXPERIMENTAL RESULTS

**4.1. Verifying the Effectiveness of the Method.** An experimental step was established for cylindrical samples made of isotropic materials according to the abovementioned method.

The testing method of axial thermal conductivity of cylindrical cores is commonly used in many industries, and relevant industry standards exist in China.<sup>31,32</sup> The cylindrical cores formed using lead had a diameter of 6.20 cm and a length of 2.88 cm, with a temperature of 32.4 °C at one end. After this temperature stabilized for 20 min, the other end was measured as 30.0 °C, and the heat flux was 8.84 W while passing through the curved heat source plate. Equation 2 presents the steady-state method to measure the end-face thermal conductivity as follows

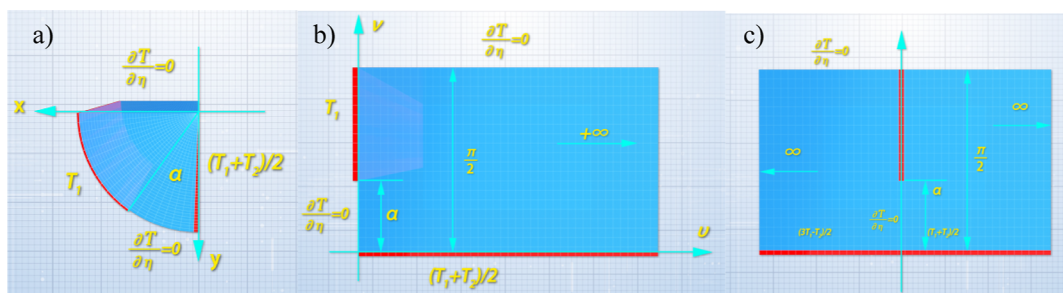


**Figure 2.** Conformal and Schwarz–Christoffel transformations. (a) Boundary conditions of a quarter circle, taken one-fourth of Figure 1b. (b) Transformed domain by conformal transformation. (c) Extension of the transformed domain by the Schwarz–Christoffel transformation.



**Figure 3.** Sketch map during experimental procedures (Jiahuan He, 2022).

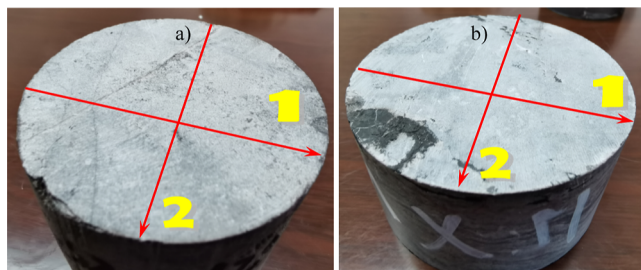


**Figure 4.** Experimental test samples and test direction (a) GS20-12 and (b) MX11–5342.34.

$$\lambda = \frac{hP}{S(T_1 - T_2)} \quad (2)$$

The axial thermal conductivity of 35.1 W/m K for this lead sample was easy to be calculated.

The radial thermal conductivity was gauged almost immediately. The purple copper foil was stuck onto two cambered surfaces toward a 90° centering angle on the circumferential surface to heat one end to 30.1 °C and subsequently check the other end as 28.6 °C after 20 min; the heat flux was 1.53 W when getting past the arched heat source

plate. The centering angle of 90° implied  $K'/K = 1$ , and the radial thermal conductivity was 35.2 W/m K, calculated using eq 1. Because the axial thermal conductivity test method is recognized in the industry, we must compare it with the results of the radial thermal conductivity test method to demonstrate its effectiveness. Overall, this measurement method for assessing radial thermal conductivity differs from conventional end-face steady-state testing by 0.3%, proving that this method is effective in principle.

**4.2. Anisotropic Testing Results.** In fact, most rocks have anisotropic properties owing to their unique formation conditions. Furthermore, some carbonate rock samples were selected to test their thermal conductivity in different radial directions (Figure 4 and Table 1).

## 5. RESULTS AND DISCUSSION

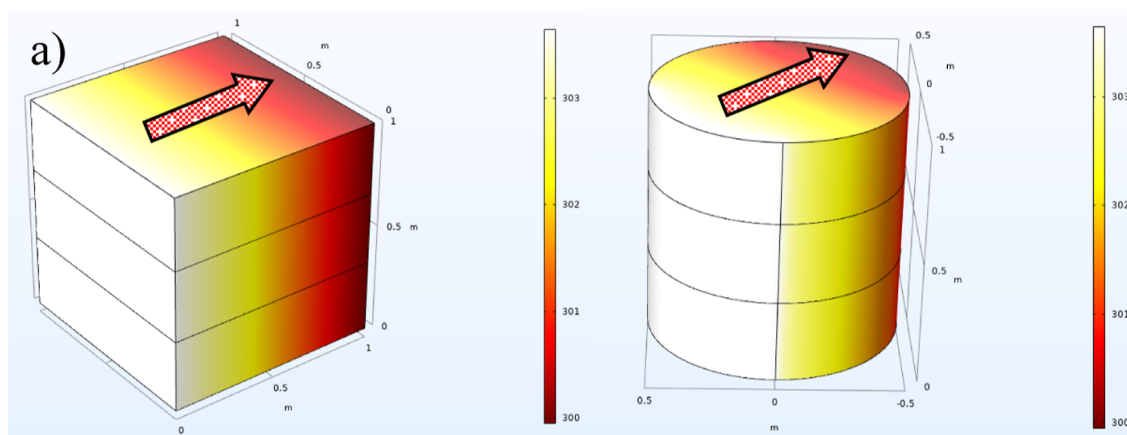
**5.1. Numerical Simulation on the Difference with Conventional Methods.** To identify a systematic error in this method for cylindrical samples due to theoretical assumptions, the measured results were compared with those of a steady-state approach for square samples. These results were simulated using the finite element method, and COMSOL Multiphysics 5.5 simulation was used to obtain a thermal field distribution. Anisotropy is omnipresent in the objective world. Additionally, as shown in Figure 5, the three most common cases are discussed.

Heat flow behaves similarly to electricity flow. Previously, researchers noted differences between radial resistivity testing and traditional methods, providing a reference for radial thermal conductivity testing.<sup>30</sup> The disparity did not exceed 10% in most cases except for some extreme conditions in cases 2 and 3.

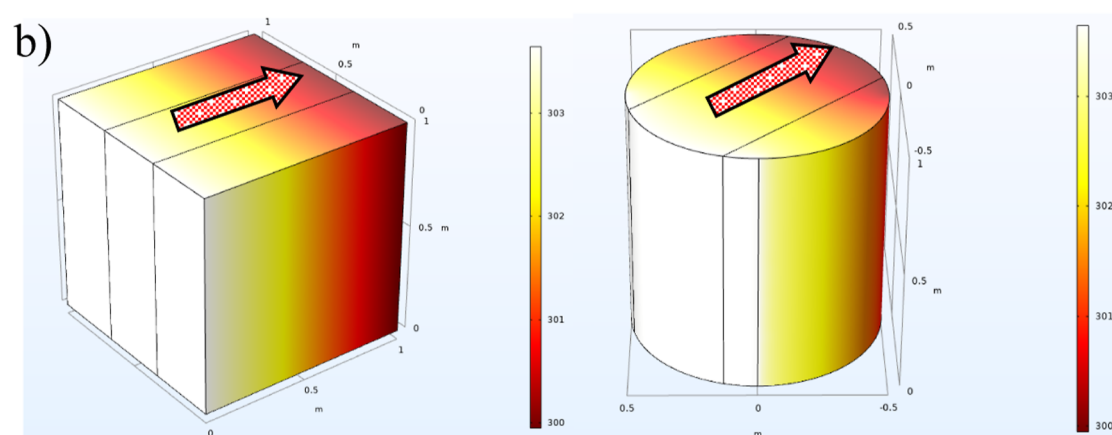
Case 2 represents one sort of samples with lower thermal conductivity; their edge parallel to the heat flow direction is coated by a few materials with higher thermal conductivity. Figure 6a shows that the conductivity is set at 1 W/m K on the right and 0.1 W/m K on the left. The simulation results show a radial thermal conductivity of 0.111 W/m K and a thermal conductivity of 0.190 W/m K for a square sample, with a difference of 41.6%. In this case, the thermal conductivity

**Table 1. Thermal Conductivity Testing Results**

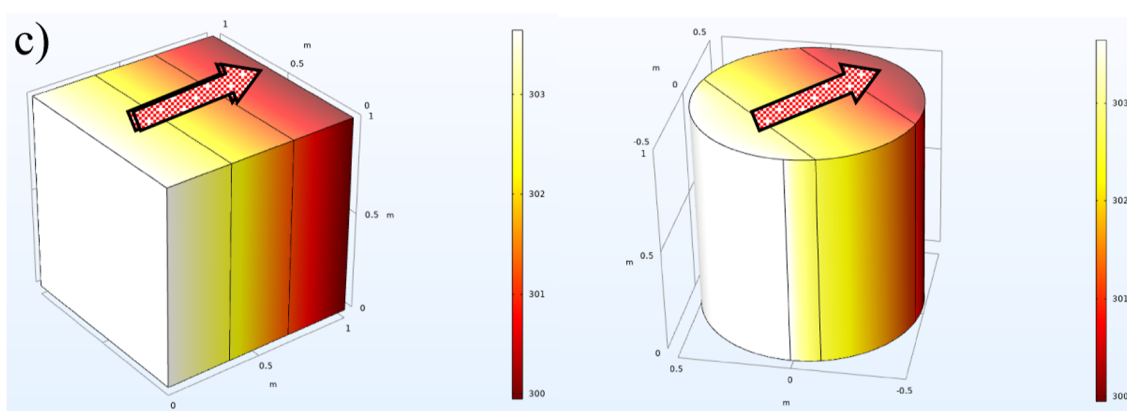
sample ID	length (cm)	diameter (cm)	heat flux (W)	direction	heat source plate temp (°C)	heat dissipation temp (°C)	thermal conductivity (W/m K)
GS20-12	6.198	6.583	0.48	1	30.5	26.8	2.09
GS20-12	6.198	6.583	0.48	2	28.9	26.3	2.76
MX11–5342.34	6.198	6.583	0.36	1	30.4	27.5	3.10
MX11–5342.34	6.198	6.583	0.36	2	28.1	25.7	3.75



Case 1



Case 2



Case 3

**Figure 5.** Radial thermal conductivity testing method corresponding to three cases;  $\theta$  is the included angle between the lamination and end planes  $a$  and  $\varphi$  is the included angle between the projection of the lamination plane on the end plane and the heat flow direction. (a) Case 1:  $\theta = 0$ ,  $\varphi = 0$ . (b) Case 2:  $\theta = \pi/2$ ,  $\varphi = 0$ . (c) Case 3:  $\theta = \pi/2$ ,  $\varphi = \pi/2$ .

measured by the radial method will be smaller than that of a rectangular parallelepiped sample to a certain extent. However,

as listed in Table 2, the discrepancy in testing results between these two methods decreases to <10% when the volume ratio

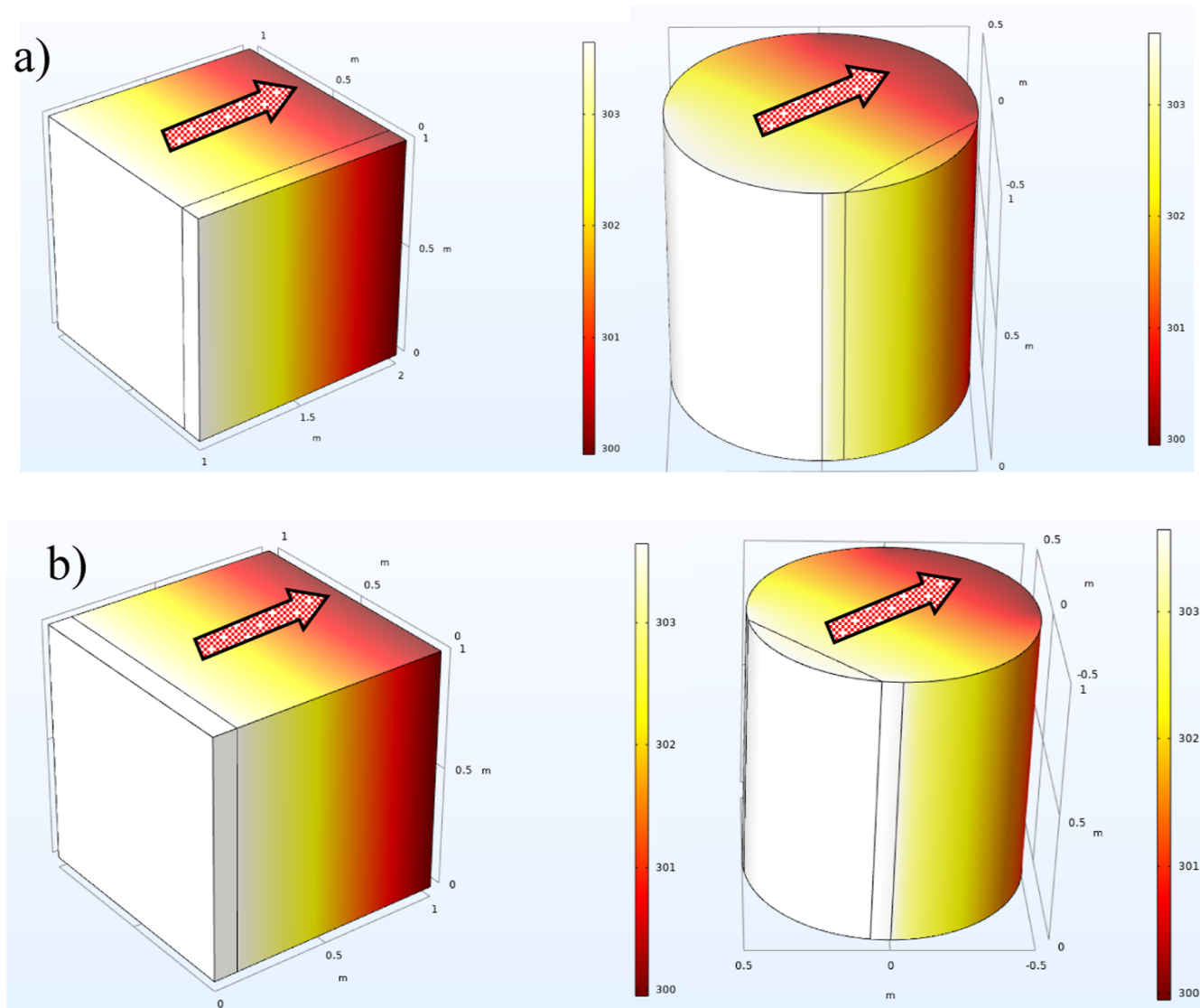


**Figure 6.** Two cases with a greater difference (a) extreme condition in case 2 and (b) extreme condition in case 3.

**Table 2. Numerical Simulation Results of Different Material Thicknesses in Case 2**

volume ratio of high conductivity to low conductivity	radial testing and simulation on thermal conductivity (W/m K)	square testing and simulation on thermal conductivity (W/m K)	systematic error (%)
9:1	0.965	0.910	6.08
7:3	0.760	0.746	1.90
5:5	0.550	0.550	0
3:7	0.334	0.370	9.72
1:9	0.111	0.190	41.6

of the high conductivity value to the low conductivity value exceeds 1:9.

In the other cases, when the thermal conductivity is high, the radial thermal conductivity is greater than that obtained using the cuboid testing method, but a fraction of thermal conductivity materials can be found at the edge perpendicular to the heat flow direction. The thermal conductivity on both the left and right sides of the sample is set to 0.1 and 1 W/m K, respectively (Figure 6b). The simulation studies show that the result from the radial thermal conductivity testing is 0.896 W/

**Table 3. Numerical Simulation Results of Different Material Thicknesses in Case 3**

volume ratio of high conductivity to low conductivity	radial testing and simulation on thermal conductivity (W/m K)	square testing and simulation on thermal conductivity (W/m K)	systematic error (%)
9:1	0.896	0.526	70.3
7:3	0.276	0.270	2.69
5:5	0.181	0.182	0.25
3:7	0.137	0.137	0.33
1:9	0.107	0.110	2.35

m K, whereas the result from thermal conductivity testing for a square sample is 0.526 W/m K, with a difference of 70.3%. However, as listed in Table 3, the difference between the two methods will decrease to less than 3% step by step when the volume ratio of high conductivity to low conductivity reduces to 7:3 or less.

To summarize, when combined with previous studies, the difference between the proposed and traditional resistivity anisotropy methods is theoretically acceptable, provided that nothing changes in the two extreme cases (the volume ratio of

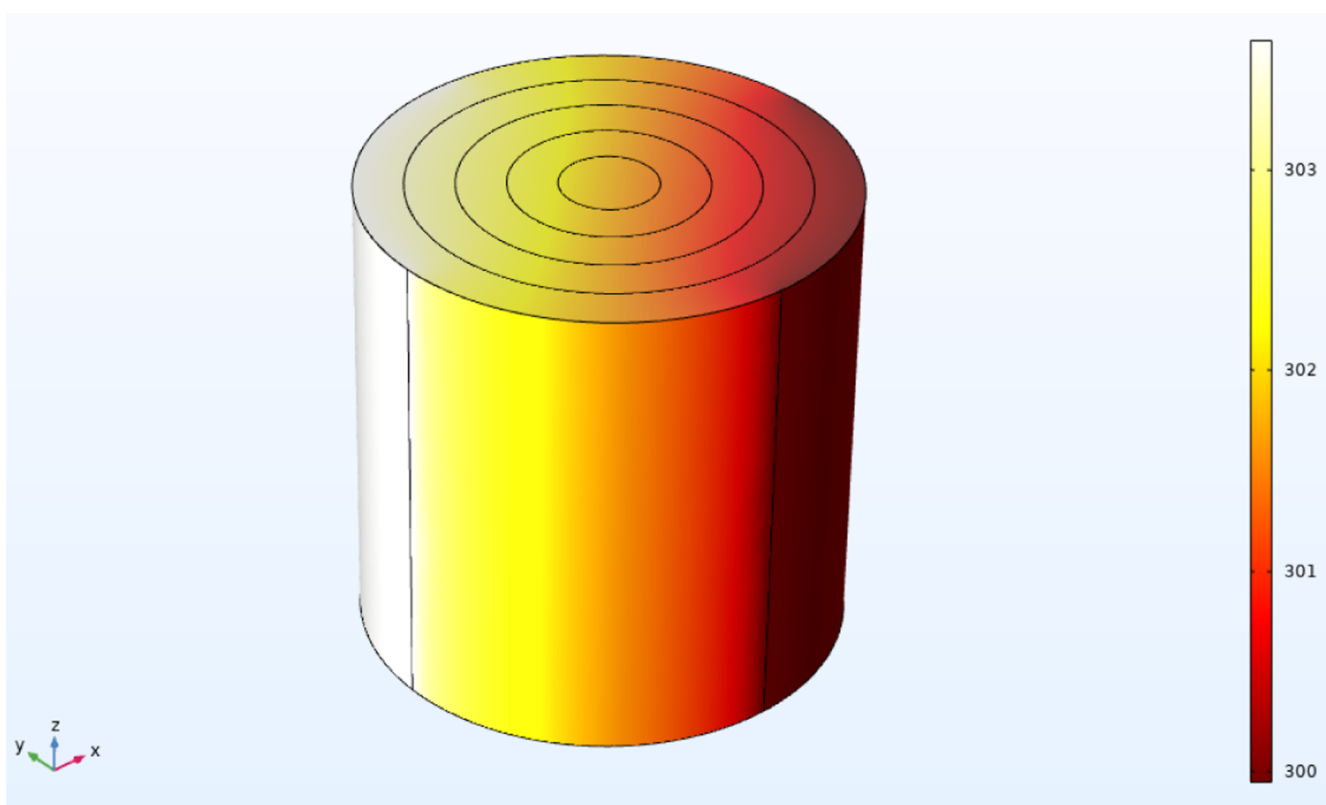


Figure 7. Numerical simulation results of a cylindrical battery.

high conductivity to low conductivity is  $<1:9$  in case 2 or  $>9:1$  in case 3) (Figure 6).<sup>29</sup>

**5.2. Error in Experimental Testing.** Sample testing and analysis exhibit a contact relation of the sample to heating and heat dissipation metal plates, which affects the accuracy of the method. Generally, if the sample does not make close contact with the sheets, the actual contact area is reduced, causing the measured thermal conductivity to be lower than the real value. At the same time, experimental conditions should be verified, that is, the conductivity of materials surrounding the sample during the testing course should be lower than that of the sample itself. Otherwise, additional heat flow may be transferred from heating to heat dissipation plates through sleeves, presenting a larger thermal conductivity than the real one. The testing error can be considered acceptable if the conductivity of sleeve materials is low enough.

Additionally, there is a concern regarding the heating capacity of the heat source. In the design phase of experimental schemes, heating capacity must be calibrated by substances with uniform properties and known heat conductivity. If heating capacity directly participates in a calculation, great damage may occur in experiments. The heating capacity value used in the calculation formula may be higher than the actual value, resulting in large heat conductivity values of tested samples. The aforementioned situation should be avoided during experiments.

**5.3. Testing Error of Cylindrical Batteries.** Cylindrical batteries are rolled inward continuously, and Figure 7 shows such characteristics. In this case, finding corresponding methods to measure square samples is difficult. The method to gauge the radial thermal conductivity is more appropriate and aligned with conditions when using complex variables. All physical parameters at the same position at each height have

the same properties. Therefore, using the proposed method to test the radial thermal conductivity is feasible in this study.

## 6. CONCLUSIONS

We developed a method for measuring radial thermal conductivity in cylindrical samples as cores and batteries may exhibit anisotropy. The computation of radial thermal conductivity depends on the heat conduction equation satisfying Fourier's law. Furthermore, a nondestructive measuring technique for the radial thermal conductivity of cylindrical samples was established using conformal and polygonal mapping in the theory of complex variables. To verify its reliability, we compared axial and radial measurements of cylindrical samples with uniform properties and established a good agreement between them. Herein, both the feasibility and adaptability of the method were confirmed via numerical simulation and theoretical analysis in various cases. The results showed that compared with other previous approaches, the nondestructive measuring method is more suitable for cores with prominent lamination features and batteries resembling nested circular rings because it can better characterize thermal conductivity anisotropy.

## AUTHOR INFORMATION

### Corresponding Author

Jiahuan He – Exploration and Development Research Institute, PetroChina Southwest Oil and Gasfield Company, Chengdu 610041, China; Shale Gas Evaluation and Exploration Key Laboratory of Sichuan Province, Chengdu 610213, China; School of Ocean and Earth Science, Tongji University, Shanghai 200092, China; [orcid.org/0000-0002-6395-5408](https://orcid.org/0000-0002-6395-5408); Email: [HeJiahuan@petrochina.com.cn](mailto:HeJiahuan@petrochina.com.cn)

## Authors

**Long Wen** – Exploration and Development Research Institute, PetroChina Southwest Oil and Gasfield Company, Chengdu 610041, China; Shale Gas Evaluation and Exploration Key Laboratory of Sichuan Province, Chengdu 610213, China

**Xiao He** – Shale Gas Evaluation and Exploration Key Laboratory of Sichuan Province, Chengdu 610213, China; PetroChina Southwest Oil and Gasfield Company, Chengdu 610051, China

**Tingting He** – Exploration and Development Research Institute, PetroChina Southwest Oil and Gasfield Company, Chengdu 610041, China

**Tangyan Liu** – School of Ocean and Earth Science, Tongji University, Shanghai 200092, China

**Qiang Kang** – Exploration and Development Research Institute, PetroChina Southwest Oil and Gasfield Company, Chengdu 610041, China

**Daocheng Wang** – PetroChina Southwest Oil and Gasfield Company, Chengdu 610051, China

**Xian Peng** – Exploration and Development Research Institute, PetroChina Southwest Oil and Gasfield Company, Chengdu 610041, China

**Hongyu Yao** – Exploration and Development Research Institute, PetroChina Southwest Oil and Gasfield Company, Chengdu 610041, China; Shale Gas Evaluation and Exploration Key Laboratory of Sichuan Province, Chengdu 610213, China

**Yin Zhang** – Exploration and Development Research Institute, PetroChina Southwest Oil and Gasfield Company, Chengdu 610041, China

**Xiaohang Deng** – Exploration and Development Research Institute, PetroChina Southwest Oil and Gasfield Company, Chengdu 610041, China; Sichuan Kelite Oil and Gas Technology Service Limited Company, Chengdu 610041, China

Complete contact information is available at:

<https://pubs.acs.org/10.1021/acsomega.2c06901>

## Notes

The authors declare no competing financial interest.

## ACKNOWLEDGMENTS

This work was financially supported by special funds for local science and technology development fund guided by the central government of Sichuan Province (no. 2020ZYD062) and the Research Project of the PetroChina Southwest Oil and Gas Field Company (no. 20220312-10).

## REFERENCES

- (1) Li, H.; Yang, Y.; Song, R.; Wang, T.; Sun, H.; Zheng, L. Adaptability of single-well downhole heat exchanger in developing mid-deep geothermal resources. *Nat. Gas Explor. Dev.* **2021**, *44*, 118–126.
- (2) Luo, N.; Zhang, J.; Li, J.; Xin, S. Development and utilization prospect of the geothermal resources in the buried hills of the Xiong'an New Area and its periphery. *Nat. Gas Ind.* **2021**, *41*, 160–171.
- (3) Yu, G.; Liu, C.; Zhang, L.; Fang, L. Parameter sensitivity and economic analyses of an interchange-fracture enhanced geothermal system. *Adv. Geo-Energy Res.* **2021**, *5*, 166–180.
- (4) Sui, Z.; Sun, M.; Zhang, D. Influence of the goal of carbon neutrality on domestic natural-gas industry and some counter-measures. *Nat. Gas Technol.* **2021**, *15*, 69.

- (5) Zhang, F.; Guo, Y.; Zhao, J.; Gong, Q. Technological input effect of China's energy industrial growth. *Nat. Gas Technol.* **2021**, *15*, 72.
- (6) Mao, X.; Guo, D.; Luo, L.; Wang, T. The global development process of hot dry rock (enhanced geothermal system) and its geological background. *Geol. Rev.* **2019**, *65*, 1462–1472.
- (7) Zhao, X.; Yan, Y.; Liu, Y.; Gao, H.; Liu, Z. Development trend and outlook of geothermal industry in the world. *World Pet. Ind.* **2020**, *27*, 53–57.
- (8) Shejiao, W.; Chen, Q.; Yan, J.; Fang, C. Development trend for geothermal energy industry and technology and suggestions on petroleum companies. *Pet. Sci. and Technol. Forum* **2020**, *39*, 9–16.
- (9) Wang, S.; Kang, R.; Feng, X.; Wang, K.; Fang, C.; Cao, Q.; Cui, Z. A optimization method of heat pump peak-shaving ratio based on economic evaluation of geothermal heating project. *Nat. Gas Ind.* **2021**, *41*, 152–159.
- (10) Wang, S.; Li, F.; Yan, J.; Hu, J.; Wang, K.; Ren, H. Evaluation methods and application of geothermal resources in oilfields. *Acta Pet. Sin.* **2020**, *41*, 554–564.
- (11) Duan, Z. F.; Li, F.; Gong, L.; Yang, Y.; Li, X. Geo-thermal development well spacing patterns based on hydrothermal coupled modeling in oil–gas bearing areas. *Nat. Gas Ind.* **2020**, *40*, 156–162.
- (12) Luo, Q.; Li, J.; Lei, X.; Xu, Q.; Dai, B.; Ma, W.; Qin, W.; Yuan, Z. Deep earth fluids: Basic characteristics and energy effects. *Nat. Gas Explor. Dev.* **2021**, *44*, 1–8.
- (13) Zhang, J.; Xie, J. Design and productivity evaluation of multi-lateral well enhanced geothermal development system. *Nat. Gas Ind.* **2021**, *8*, 402.
- (14) Lin, Z.; Liu, K.; Liu, J.; Geng, D.; Ren, K.; Zheng, Z. Numerical model for geothermal energy utilization from double pipe heat exchanger in abandoned oil wells. *Adv. Geo-Energy Res.* **2021**, *5*, 212–221.
- (15) Li, B.; Alexey, S. Decoupled approximation and separate extrapolation of P- and SV-waves in transversely isotropic media. *Geophysics* **2021**, *86*, C133–C142.
- (16) Alarouj, M.; Matthew, D. J. Numerical modeling of self-potential in heterogeneous reservoirs. *Geophysics* **2022**, *87*, E103–E120.
- (17) Sun, Q.; Zhang, R.; Chen, K.; Feng, N.; Hu, Y. Anisotropic modeling with geometric multigrid preconditioned finite-element method. *Geophysics* **2022**, *87*, A33–A36.
- (18) Safanda, J. Effect of thermal conductivity anisotropy of rocks on the subsurface temperature field. *Geophys. J. Int.* **2010**, *120*, 323–330.
- (19) Deming, D. Estimation of the thermal conductivity anisotropy of rock with application to the determination of terrestrial heat flow. *J. Geophys. Res.* **1994**, *99*, 22087–22091.
- (20) Pribnow, D.; Sass, J. Determination of thermal conductivity for deep boreholes. *J. Geophys. Res.* **1995**, *100*, 9981–9994.
- (21) Murashko, K. A.; Pyrhonen, J.; Jokiniemi, J. Determination of the through-plane thermal conductivity and specific heat capacity of a Li-ion cylindrical cell. *Int. J. Heat Mass Transfer* **2020**, *162*, 120330.
- (22) Yang, W.; Wang, Y.; Liu, J.; Liu, D. A review of thermal conductivity by means of the guarded-hot-plate apparatus. *J. Xi'an Univ. Archit. Technol.* **2018**, *50*, 57–64.
- (23) Carmona, M.; Eduar, P.; Mario, P. Experimental evaluation of porosity, axial and radial thermal conductivity, of an adsorbent material composed by mixture of activated carbon, expanded graphite and lithium chloride. *Appl. Therm. Eng.* **2019**, *150*, 456–463.
- (24) Drake, S. J.; Wetz, D. A.; Ostanek, J. K.; Miller, S. P.; Heinzl, J. M.; Jain, A. Measurement of anisotropic thermophysical properties of cylindrical Li-ion cells. *J. Power Sources* **2014**, *252*, 298–304.
- (25) Ahmed, M. B.; Salwa, S.; Ankur, J. Measurement of radial thermal conductivity of a cylinder using a time-varying heat flux method. *Int. J. Therm. Sci.* **2018**, *129*, 301–308.
- (26) He, J.; Li, M.; Zhou, K.; Zeng, L.; Li, N.; Yang, Y.; Xiao, D.; Huang, M. Radial resistivity measurement method for cylindrical core samples. *Interpretation* **2020**, *8*, 1071–1080.
- (27) Tiari, S.; Addison, H. An experimental study on the effect of annular and radial fins on thermal performance of a latent heat thermal energy storage unit. *J. Energy Storage* **2021**, *44*, 103541.

(28) Collins, R. E. Determination of the transverse permeabilities of large core samples from petroleum reservoirs. *J. Appl. Phys.* **1952**, *23*, 681–684.

(29) Muskat, M.; Wyckoff, R. D.; Botset, H. G.; Meres, M. W. Flow of gas-liquid mixtures through sands. *Trans. Am. Inst. Min. Metall. Pet. Eng.* **1937**, *123*, 69–96.

(30) He, J.; Liu, T.; Wen, L.; He, T.; Li, M.; Li, J.; Wang, L.; Yao, X. Numerical simulation analysis of difference from a radial resistivity testing method for cylindrical cores and a conventional testing method. *Mathematics* **2022**, *10*, 2885.

(31) Wang, B.; Ma, A.; An, B.; Gao, L.; Cai, C.; Wang, P.; Guo, Q.; Xie, Y.; Li, G.; Xie, H.; Zhang, J.; Gao, H.; Tang, L.; Chen, J.; Fang, Q.; Wu, H.; Zhou, X. *Test Method for Effective Thermal Conductivity of Wall Materials*; National Standards of the People's Republic of China, GB/T 32981-2016, 1988; pp 1–9.

(32) Standards of the Ministry of Electronic Industry of the People's Republic of China. *Test Method for Properties of Thermoelectric Cooling Materials: Thermal Conductivity Test Method*; Standards of the Ministry of Electronic Industry of the People's Republic of China, SJ 2857.1-88, 1988; pp 1–5.